Supporting Information

Fasano et al. 10.1073/pnas.1012071107

SI Materials and Methods

Mouse Studies. Generation of Ras-guanine nucleotide-releasing factor 1 (GRF1)–KO mice has been described (1, 2). Ras-GRF1–KO and littermate controls were kept in mix background (C57BL/6 × 129SVJ) and housed under a 12-h light/dark cycle with ad libitum access to the food.

Lesion Surgery. Ras-GRF1 WT (n = 20) and KO (n = 20) mice were anesthetized with isofluorane (Baxter Medical AB) and secured in a stereotaxic frame equipped with a mouse adaptor. One microliter of 6-hydroxydopamine (6-OHDA)-HCl (3 μg/μL) was injected into the right ascending medial forebrain bundle at the following coordinates according to the mouse brain atlas: AP −0.7; L −1.2; DV −4.7 from the dural surface using a glass capillary attached to a 10-μL Hamilton syringe. Severity of dopamine denervation was assessed at the end of the experiments analyzing striatal levels of tyrosine hydroxylase (TH) and nigral cell loss using immunohistochemical labeling.

Motor Impairment and Induction of Abnormal Involuntary Movements. Mice were evaluated in the open field 2 wk after lesion to estimate the success rate of lesioning. Starting from day 18, mice were treated twice a day, for 9 consecutive days with an escalating L-dopa dosing regimen (1.5, 3, and 6 mg/kg) plus benserazide (12 mg/kg) (Ras-GRF1 WT, n = 9; Ras-GRF1–KO, n = 9) or with saline (Ras-GRF1 WT, n = 6; Ras-GRF1–KO, n = 6). In a second experiment, the same protocol of increasing L-dopa treatment was applied in combination with a low dose (10 mg/kg) of the MEK inhibitor, SL327. Abnormal involuntary movements (AIMs) were scored using a 0–4 rating scale according to validated mouse model of L-dopa–induced dyskinesia (LID) (3). Every morning, mice were placed individually in large transparent boxes and observed for 1 min every 20th min during 180 min after L-dopa injection.

Immunohistochemistry. Following transcardiac perfusion with 4% paraformaldehyde (PFA) in PBS, postfixation, cryopreservation, and storage in cryoprotective solution at −20 °C, 40-μm–thick free-floating sections were incubated overnight at 4 °C with primary antibodies [TH, 1:1,000 (Pel-Freez Biologicals); Phospho-p44/42 MAP kinase, 1:200 (Cell Signaling), and FosB sc-48, 1:15,000 (Santa Cruz Biotechnology)]. Sections then were incubated with appropriate biotinylated secondary antibodies (Vector Labs) for 2 h. Tissue sections were processed further using Vectastain ABC kit (Vector Labs) and DAB detection. The TH-positive fiber density was quantified using Image J software (version1.39u). pERK- and FosB-positive neurons were counted from dorsolateral striatum, in four sections per mouse, bilaterally. All visible positive nuclei or cell bodies within a field were counted and expressed as number of cells per square millimeter. Estimation of nigral cell loss was assessed by quantifying the average TH-immunopositive neurons in the substantia nigra pars compacta (SNc) at two different levels for each animal. The number of TH-positive neurons was counted bilaterally on at least two sections at each level. All positive neurons lying outside a vertical line passing through the accessory optical tract were counted on each side.

Immunofluorescence. Sections from M4- and A2A-EGFP mice were incubated overnight with a rabbit polyclonal antibody against Ras-GRF1 (1:100; Santa Cruz Biotechnology) and then for 1 h with a Trich-coupled secondary antibody (Sc-2780, 1:200; Santa Cruz Biotechnology). EGFP-labeled neurons were visualized by direct detection of endogenous fluorescence. Nuclei were counterstained by incubation with DAPI for 5 min.

Free-floating sections from LV-injected mice were incubated overnight at 4 °C with an anti-GFP rabbit conjugate antibody (Alexa Fluor 488, 1:500; Invitrogen) and a polyclonal antibody against Phospho-p44/42 MAP kinase (1:200) (Cell Signaling Technology) followed by incubation with a biotinylated secondary antibody (1:200; Vector Laboratories) and Extravidin-Cy3 (1:1,000; Sigma). Images from saline- and cocaine-challenged animals were acquired with a Leica TCS SP2 laser scanning confocal microscope, and the number of LV/pERK-positive neurons was counted.

Western Blotting. After cervical dislocation, the striata were dissected and homogenized in lysis buffer. Protein extracts were separated onto SDS/PAGE, transferred to nitrocellulose membrane, and incubated with antibodies against Ras-GRF1 protein (1:1,000; α-PH home-made, see ref. 1), Ras-GRF2-C20 (1:1,000; Santa Cruz Biotechnology), Phospho-p44/42 MAP kinase (1:1,000; Cell Signaling), and GAPDH (FL-335): sc-25778 (1:1,000; Santa Cruz Biotechnology). The immunoblots were analyzed with Image J software to measure the optical density of the bands, using GAPDH as loading control. Normalized Ras-GRF1, Ras-GRF2, and phosphorylated ERK2 (pERK2) intensities were obtained by determining the signal-to-noise ratio using a saline intact striatum as a reference.

In Situ Hybridization. In situ hybridization histochemistry was performed as described recently (4) using a probe that specifically recognizes Δ*fosB* mRNA. Briefly, synthetic oligomers were labeled at the 3′ end with 4 M [^{35}S] deoxyadenosine 5′-triphosphate (37 TBq/mmol) (Amersham Pharmacia Biotech) using 15 U of terminal deoxynucleotidyl transferase (Amersham Pharmacia Biotech). An amount of ^{35}S-labeled probe equivalent to 107 cpm/mL buffer was added to the hybridization buffer. Hybridized sections were exposed to Fuji imaging plates (Fujifilm AB) for 1–12 h and then scanned in a BAS 5000 phosphoimager (Fujifilm AB) to obtain digitized autoradiographs. The hybridization signal was analyzed in the medial and lateral part of the caudate-putamen using the program TINA (Fujifilm AB).

Lentiviral Vector Production and Stereotaxic Injection in the Mouse. The ERK2^{K52R} mutant has been described already (5). The two dominant-negative constructs, Ras-GRF1-NR2B-BD and Ras-GRF1-CD^{W1056E}, were designed using the human Ras-GRF1 sequence and adapted from the mouse and rat sequences (6, 7). In vivo visualization of the transgene was obtained by a concomitant GFP expression from the same hPGK promoter using an internal ribosomal entry site. High-titer production of lentiviral vectors (LV) was achieved by standard transfection methods in HEK293T cells, as previously described (5, 8, 9). Unilateral stereotaxic injections of LVs were performed in 8-wk-old anesthetized mice placed in a stereotaxic frame. One microliter of either targeting LV or control LV-GFP was injected into the motor dorsal striatum.

Monkey Studies. All experiments were carried out under veterinarian supervision in accordance with the European Communities Council Directive of November 24, 1986, (86/609/EEC) for the care of laboratory animals in a facility accredited by the Association for Assessment and Accreditation of Laboratory Animal Care. We used nine female rhesus monkeys (*Macaca mulatta*; Xierxin) housed in individual primate cages (1.1 m ×

0.8 m × 1 m) with controlled humidity, temperature, and light (12-h light/dark cycle); food and water were available ad libitum.

Experimental Parkinsonism. Parkinsonism and dyskinesia were induced, as described (10–12), in six monkeys. Monkeys received daily i.v. injections of 1-methyl-4-phenyl-1,2,3,6-tetrahydropyridine (MPTP) hydrochloride (0.2 mg/kg) until they displayed parkinsonian symptoms (15 ± 1 injections) (13). Within 8 wk bilateral parkinsonian syndrome stabilized (demonstrated by a constant disability score in 2 consecutive weeks). Parkinsonian monkeys were treated p.o. twice daily with Modopar (L-dopa/carbidopa, ratio 4:1) (Roche) for 6 mo at doses (15–20 mg/kg) individually adjusted to reverse the parkinsonian symptoms fully. All monkeys developed dyskinesia. Three additional drug-naïve unlesioned monkeys were used as controls for immunohistochemical validations.

Stereotaxic Surgery. Because individual macaques differ, the standard Horsley–Clarke technique was improved by using sagittal and frontal ventriculography to locate the borders of the third ventricle and the edges of the anterior and posterior commissures (10, 12, 14). Surgeries were performed using a convection-enhanced delivery method (Unimecanique microinjector) with a mixture (1:1:1) of the three vectors previously validated in the mouse model at two rostro-caudal levels (50 μL at each level), i.e., at the anterior commissure (AC) (AC 0 mm) and 3 mm caudal to AC (AC −5 mm), 1 mm above the virtual horizontal line passing through the AC and posterior commissural (10, 12). After each injection the syringe was left in place for 10 min to prevent leakage.

Behavioral Experiments. Monkeys' response to L-dopa was measured before virus injection. Starting at 8 wk postsurgery, animals were assayed every 2 d for behavioral responses to their tailored dose of L-dopa, the D1 agonist SKF 38393 (1.5 mg/kg, s.c.) (14), and the D2/D3 agonist quinpirole (1.5 mg/kg, s.c.) (14). Monkeys were videotaped in an observation cage (1.1 m × 1.5 m × 1.1 m) for 60 min before and 240 min after drug administration and scored on a parkinsonian monkey rating scale (0, normal; >6, parkinsonian animal) (10–12). Dyskinesia was rated on the Dyskinesia Disability Scale: 0, dyskinesia absent; 1, mild and rare dyskinetic postures and movements; 2, moderate abnormal movements, not interfering significantly with normal behavior; 3, marked frequent dyskinesia affecting normal activity; 4, severe, disabling, virtually continuous dyskinetic activity replacing normal behavior. Locomotor activity was measured concomitantly every 5 min with infrared activity monitors (10, 12).

Postmortem Processing. Monkeys were deeply anesthetized by sodium pentobarbital (150 mg/kg, i.v.) 1 h after the last vehicle or L-dopa injection and then were perfused transcardially with a mixture of 2% PFA and 0.2% glutaraldehyde in phosphate buffer (0.1 M) (15). Sections 40-μm thick were incubated with rabbit anti-GFP antibody (1:5,000) (Invitrogen), mouse anti-pERK antibody (1:250) (Sigma), and rabbit anti-ΔFosB antibody (1:250) for 2 d at RT and then at RT for 40 min with Dako EnVision+ system HRP-labeled polymer anti-mouse or anti-rabbit, respectively. Immunoreactivity was visualized by DAB-nickel (0.05% with 0.01% H_2O_2). Negative controls were incubated without primary antibodies. Brain sections were examined using the Mercator image analysis system (Explora Nova). Camera aperture, magnification, light power, and exposure time were fixed for all images. An examiner blind with regard to the experimental condition analyzed three representative striatal sections per immunolabeling for each animal.

Extent of lesion was checked by counting the number of TH-immunopositive neurons in the SNc and the striatal TH immunostaining. Lesion extents were similar in the two MPTP-treated groups, as previously shown (16), with a nearly complete lesion, in contrast with control animals (Fig. 3*A*).

Statistical Analyses. Global AIMs scores were analyzed by two-way ANOVA for repeated measures, and relevant differences within or between groups were analyzed pairwise by Tukey's highly significant difference (HSD) test. Counts of immunoreactive cells in the intact and lesioned striatum were analyzed by two-factor ANOVA followed by Tukey's test. The analyses were done using SPSS statistics software.

1. Brambilla R, et al. (1997) A role for the Ras signalling pathway in synaptic transmission and long-term memory. *Nature* 390:281–286.
2. Fasano S, et al. (2009) Ras-guanine nucleotide-releasing factor 1 (Ras-GRF1) controls activation of extracellular signal-regulated kinase (ERK) signaling in the striatum and long-term behavioral responses to cocaine. *Biol Psychiatry* 66:758–768.
3. Lundblad M, Picconi B, Lindgren H, Cenci MA (2004) A model of L-DOPA-induced dyskinesia in 6-hydroxydopamine lesioned mice: Relation to motor and cellular parameters of nigrostriatal function. *Neurobiol Dis* 16:110–123.
4. Valastro B, Andersson M, Lindgren HS, Cenci MA (2007) Expression pattern of JunD after acute or chronic L-DOPA treatment: Comparison with deltaFosB. *Neuroscience* 144:198–207.
5. Vantaggiato C, et al. (2006) ERK1 and ERK2 mitogen-activated protein kinases affect Ras-dependent cell signaling differentially. *J Biol* 5:14.1–14.15.
6. Krapivinsky G, et al. (2003) The NMDA receptor is coupled to the ERK pathway by a direct interaction between NR2B and RasGRF1. *Neuron* 40:775–784.
7. Vanoni M, et al. (1999) Characterization and properties of dominant-negative mutants of the ras-specific guanine nucleotide exchange factor CDC25(Mm). *J Biol Chem* 274:36656–36662.
8. Papale A, Cerovic M, Brambilla R (2009) Viral vector approaches to modify gene expression in the brain. *J Neurosci Methods* 185:1–14.
9. Indrigo M, Papale A, Orelllana D, Brambilla R (2010) Lentiviral vectors to study the differential function of ERK1 and ERK2 MAP kinases. *Methods Mol Biol* 661:205–220.
10. Berton O, et al. (2009) Striatal overexpression of DeltaJunD resets L-DOPA-induced dyskinesia in a primate model of Parkinson disease. *Biol Psychiatry* 66:554–561.
11. Bézard E, et al. (2003) Attenuation of levodopa-induced dyskinesia by normalizing dopamine D3 receptor function. *Nat Med* 9:762–767.
12. Gold SJ, et al. (2007) RGS9-2 negatively modulates L-3,4-dihydroxyphenylalanine-induced dyskinesia in experimental Parkinson's disease. *J Neurosci* 27:14338–14348.
13. Bezard E, Brotchie JM, Gross CE (2001) Pathophysiology of levodopa-induced dyskinesia: Potential for new therapies. *Nat Rev Neurosci* 2:577–588.
14. Boraud T, Bezard E, Bioulac B, Gross CE (2001) Dopamine agonist-induced dyskinesias are correlated to both firing pattern and frequency alterations of pallidal neurones in the MPTP-treated monkey. *Brain* 124:546–557.
15. Nadjar A, et al. (2006) Phenotype of striatofugal medium spiny neurons in parkinsonian and dyskinetic nonhuman primates: A call for a reappraisal of the functional organization of the basal ganglia. *J Neurosci* 26:8653–8661.
16. Guigoni C, et al. (2005) Levodopa-induced dyskinesia in MPTP-treated macaques is not dependent on the extent and pattern of nigrostrial lesioning. *Eur J Neurosci* 22: 283–287.

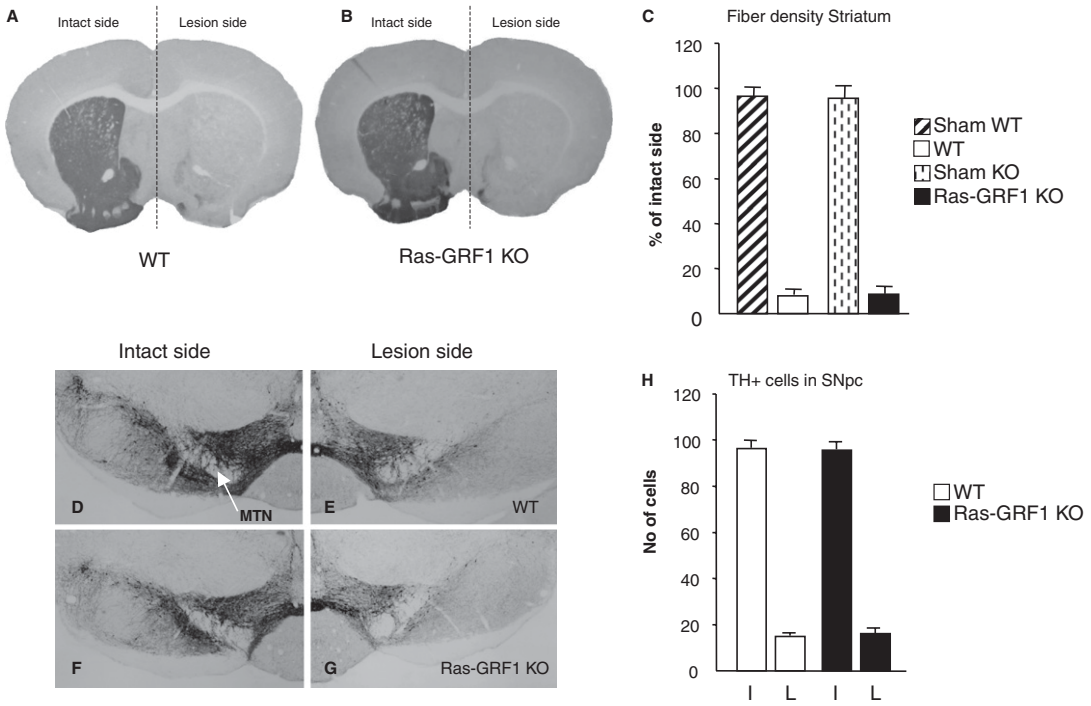

Fig. S1. Severe dopamine depletion induced by 6-OHDA lesion in WT and Ras-GRF1 KO–mice. (*A* and *B*) TH–positive staining in the intact striatum from (*A*) WT and (*B*) Ras-GRF1–KO mice. After a 6-OHDA lesion was made in the medial forebrain bundle, a profound loss of dopamine fiber in the striatum was observed (right side of the slice). (*C*) The TH optical density was measured throughout the striatum, and values are expressed as a percentage of the optical density on the intact side in sham and lesioned animals. More than 90% reduction of TH-positive fiber density was seen in lesioned animals without a difference in genotype ($P > 0.5$). (*D*–*G*) TH-positive neurons were counted in three adjacent SNc sections per animal, and only sections in which the lateral part of the substantia nigra was clearly separated by the medial terminal nucleus (MTN) were selected. (*H*) In both groups, no significant difference was seen in the number (mean ± SEM) of TH-positive cells in the intact (I) and lesion (L) side.

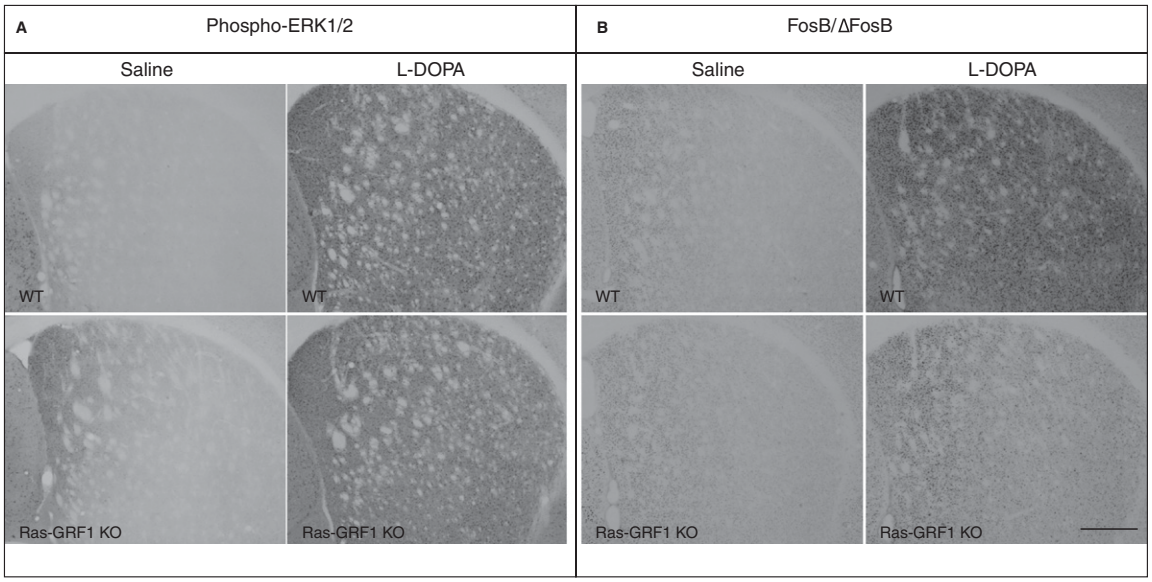

Fig. S2. Reduced distribution pattern of pERK1/2 and Fos/ΔFosB immunoreactivity in denervated Ras-GRF1–KO mice after 9 d of L-dopa treatment. (*A*) Photomicrographs of cells expressing pERK1/2 in the depleted striatum of WT (*Upper*) and Ras-GRF1–KO (*Lower*) mice after saline or L-dopa injections. (*B*) FosB/ΔFosB-positive cells in depleted striatum of WT (*Upper*) and Ras-GRF1–KO (*Lower*) mice after saline or L-dopa injection. (Scale bar: 1 mm.)

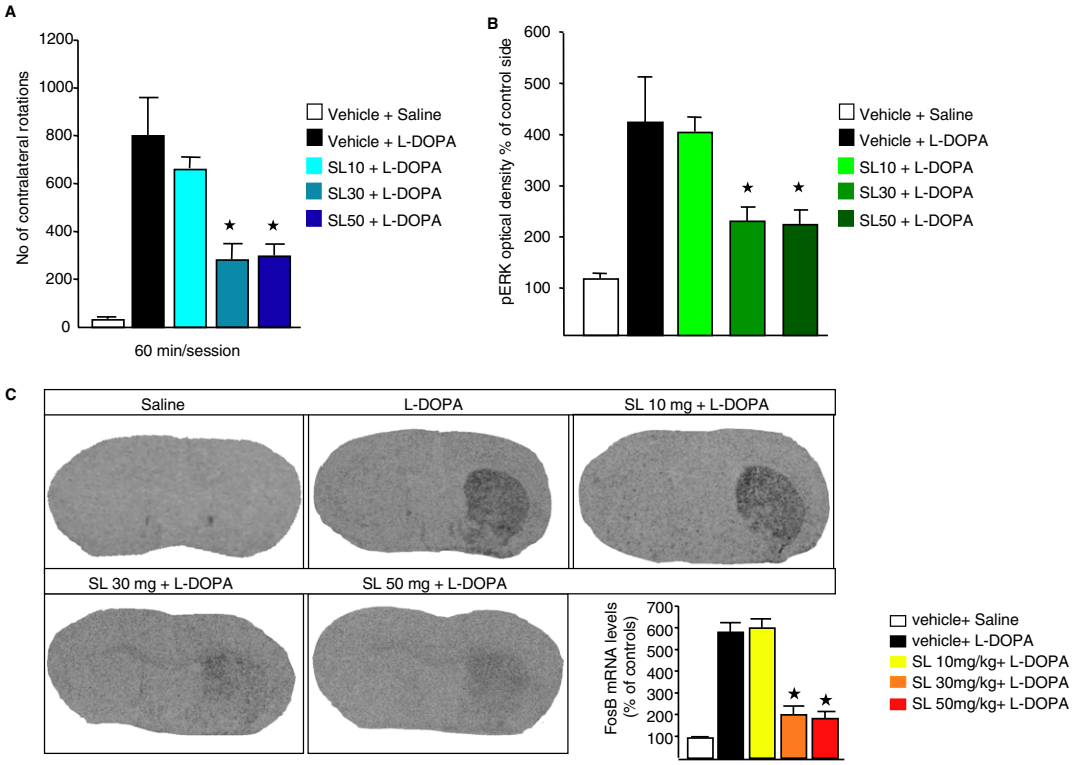

Fig. S3. A low dose of the MEK inhibitor SL327 did not alter motor responses and cellular events in 6-OHDA–lesioned mice acutely treated with L-dopa. Lesioned animals were injected with a low, medium, or high dose of SL327 (10, 30, or 50 mg/kg, respectively) or vehicle 30 min before a challenge with L-dopa (6 mg/kg). (*A*) Contralateral rotations were counted during a 60-min session. The 30- and 50-mg/kg doses of the MEK inhibitor strongly decreased L-dopa–induced turning behavior, but the lowest dose was ineffective (one-way ANOVA and post hoc Tukey's HSD test; vehicle + L-dopa vs. SL327 30 mg/kg + L-dopa and vehicle + L-dopa vs. SL327 50 mg/kg + L-dopa, $^{\star}P < 0.001$). (*B*) Coronal sections from mice killed 20 min after L-dopa injection were immunostained for pERK1/2, and optical density was analyzed. The medium and the highest dose of SL327 clearly inhibited ERK activation in lesioned striata (one-way ANOVA and post hoc Tukey's HSD test; vehicle + L-dopa vs. SL327 30 mg/kg + L-dopa and vehicle + L-dopa vs. SL327 50 mg/kg + L-dopa, $^{\star}P < 0.01$). (*C*) Representative autoradiographs showing distribution pattern of FosB mRNA in striatal sections of animals killed 3 h after L-dopa injection. The dopamine-depleted striatum is shown to the right in all panels. As expected, FosB mRNA levels were significantly induced ipsilateral to the lesion after L-dopa administration. This treatment effect was maintained in combination with 10 mg of SL327 but was markedly reduced with the other two doses (one-way ANOVA and post hoc Tukey's HSD test; vehicle + L-dopa vs. SL327 30 mg/kg + L-dopa, $^{\star}P < 0.001$; vehicle + L-dopa vs. SL327 50 mg/kg + L-dopa, $^{\star}P < 0.001$).

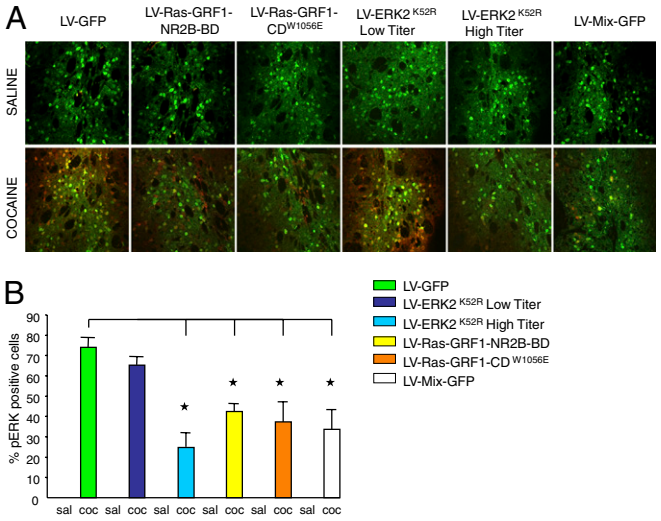

Fig. S4. Dominant-negative LV constructs were able to reduce ERK activation in mouse striatum. (*A*) WT mice received stereotaxic injections of LV-GFP, LV-Ras-GRF1-NR2B-BD, LV-Ras-GRF1-CD ^{W1056E}, LV-ERK2^{K52R} (low or high titer), or LV-Mix-GFP into the right dorsal striatum. Four weeks after surgery, mice were injected i.p. with saline (*Upper*) or 20 mg/kg of cocaine (*Lower*) and were perfused 20 min later. Brain sections were immunostained with an anti-GFP antibody (green) to label LV expression and pERK (red). (*B*) The graph shows the percentage of pERK/GFP double-positive neurons. Saline injection did not elicit ERK activation in any experimental group. Upon cocaine challenge, pERK was maximal in the LV-GFP and in the LV-ERK2^{K52R} low-titer groups, whereas ERK activation was significantly reduced in all Ras-GRF1 dominant-negative constructs and in the LV-ERK2^{K52R} high-titer groups as well as in the LV-Mix-GFP group (paired *t* tests; LV-GFP vs. LV-Ras-GRF1-NR2B-BD, $^{\star}P < 0.0001$; LV-GFP vs. LV-Ras-GRF1-CD ^{W1056E}, $^{\star}P < 0.000$; LV-GFP vs. LV-ERK2^{K52R} high titer, $^{\star}P < 0.0001$; LV-GFP vs. LV-Mix-GFP, $^{\star}P < 0.0001$). Coc, cocaine; sal, saline.

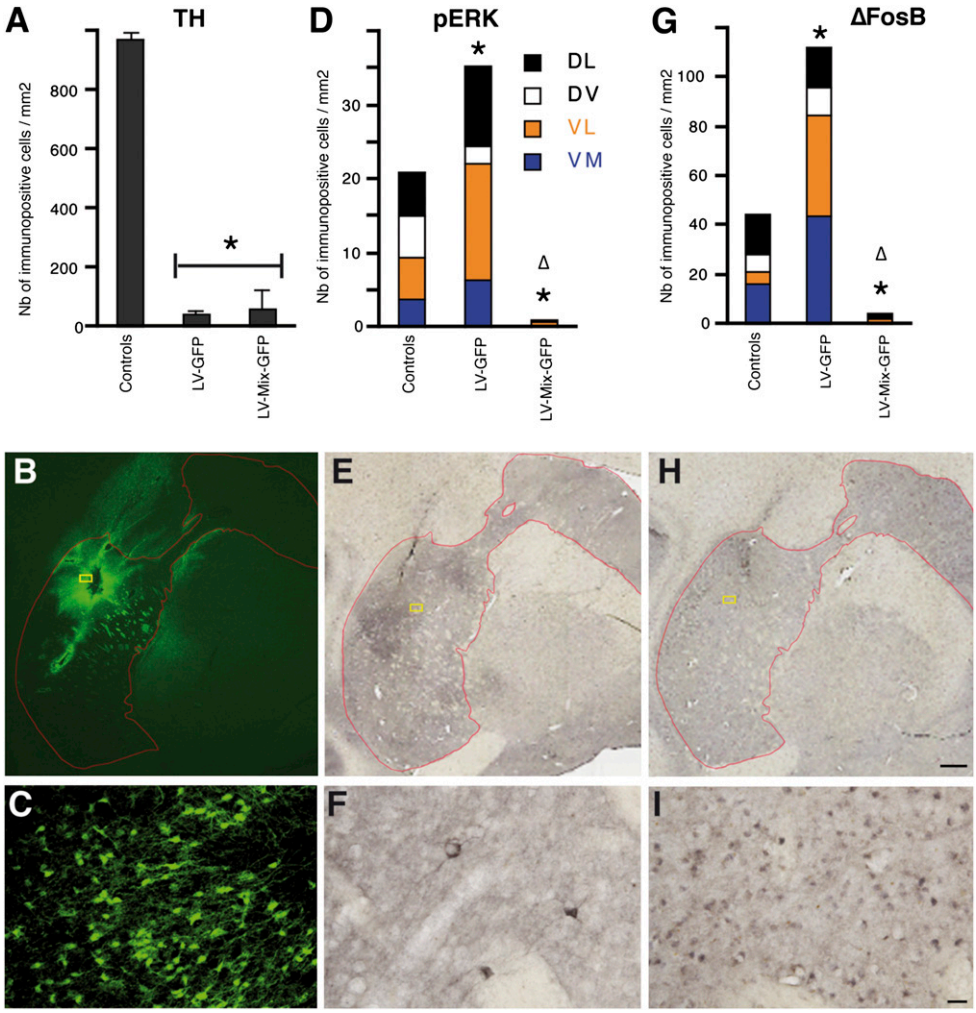

Fig. S5. Immunohistological analysis of macaque striata infected with LV-Mix-GFP. (*A*) The LV-infected MPTP-treated groups had similar extensive lesion of nigrostriatal pathway, as evidenced by the dramatic decrease in the number of TH-immunopositive neurons in the SNc in comparison with drug-naïve, unlesioned control monkeys (unpaired *t* test; $*P < 0.01$ vs. controls). The extent of transduction covered the whole motor putamen (*B*) with strong GFP expression in medium spiny neurons (*C*). Although the LV-GFP group showed the expected significant increase in the number of pERK- (*D*) and ΔFosB- (*G*) immunopositive neurons in comparison with drug-naïve, unlesioned control monkeys, the LV-Mix-GFP group showed a dramatic significant reduction of both parameters in comparison with both control and LV-GFP groups, suggesting that LV-Mix-GFP significantly dampened the Ras–ERK signaling cascade (unpaired *t* test; $*P < 0.01$ vs. controls; $^{\Delta}P < 0.01$ vs. LV-GFP). *E* and *H* show representative macroscopic views of the striatum with borders highlighted in red. (Scale bar in *H*: 1 mm.) The yellow rectangles in *E* and *H* indicate the magnified areas depicted in *F* and *I*, respectively. (Scale bar in *I*: 20 μm.)